Transport coefficients of simple fluids with steeply repulsive potentials

D M Heyes

Department of Chemistry, University of Surrey, Guildford GU2 5XH, UK

Abstract. We calculate the transport coefficients of steeply repulsive inverse power, r^{-n}, potential fluids using the Green–Kubo time correlation function method. We have explored the effect of potential steepness on the transport coefficients of these model fluids as they approach the hard-sphere limit. We have found that, even with an inverse power potential index, $n = 144$, there are still noticeable differences in some of the properties when compared with the hard-sphere fluid at the same number density. The compressibility factor, shear viscosity and thermal conductivity are some 5–10% lower than the hard-sphere value, although the self-diffusion agrees well with the hard-sphere value for $n > 72$.

1. Introduction

Molecular dynamics (MD) computer simulation has been a useful tool for probing the influence of interaction potential on the transport coefficients of model simple liquids. Notable among these studies has been those of the hard-sphere fluid (Alder *et al* 1970) and the Lennard-Jones (LJ) fluid by Levesque *et al* (1973). Most of the studies involving a continuous potential have used analytic forms suitable for simple molecular liquids. Recently there has been interest in applying MD simulation with considerably more steeply repulsive interaction potentials which are close to being hard spheres, as more realistic models for colloidal dispersions (Melrose and Heyes 1993) and granular assemblies (Langston *et al* 1994). These real systems have interaction potentials that are extremely steep on the scale of the particle diameter (much steeper than for typical molecular liquids) and are therefore very *close* to being hard spheres. It is therefore of interest to understand how the properties of these steeply repulsive systems differ from and approach those of the hard-sphere system. How steep does the potential have to become before the properties of the fluid are statistically indistinguishable from those of the hard-sphere system itself? This is the subject of this study. As part of our study of the behaviour of these systems, in a previous publication (Heyes and Aston 1993), we investigated the dependence of the elastic moduli on the steepness of the potential and discovered that they diverge in the hard-sphere limit as $\sim n$ for the inverse power potentials

$$\phi(r) = \epsilon(\sigma/r)^n \tag{1}$$

where σ is some characteristic distance and ϵ sets the energy scale for interaction between the particles. (The hard-sphere interaction is (1) in the $n \to \infty$ limit.) Associated with this result, for the shear viscosity, η_s, we also concluded that the time correlation function for the interaction part of the transport coefficients must decay infinitely rapidly as $n \to \infty$. This
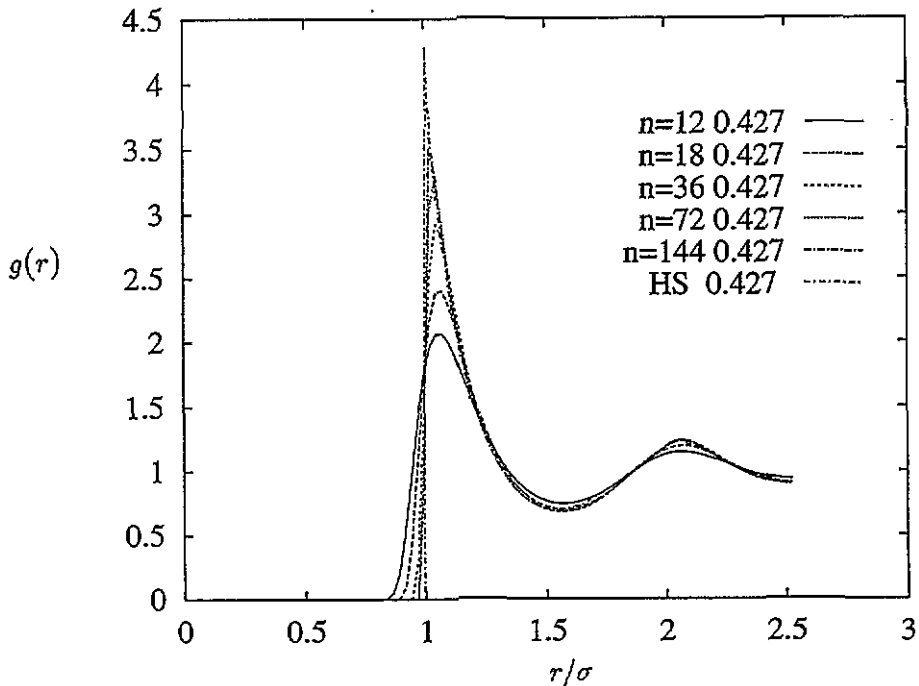
Figure 1. The pair radial distribution function for the inverse power potential for several inverse power exponents and that of the hard-sphere fluid. The key is on the figure.

is necessary to compensate for the divergence in the interaction part of the shear rigidity modulus, G_∞, in order to maintain a finite value for the shear viscosity. Here we develop the subject of the previous study and explore in greater detail the effect of the value of n on the transport coefficients of 'inverse power' simple fluids. In the previous study we only looked at η_s to a small extent. Here we also consider the self-diffusion coefficient and the thermal conductivity, and their dependence on the value of n.

We compute numerically the velocity autocorrelation function, $C_v(t)$

$$C_v(t) = \langle v_i(0)v_i(t)\rangle \tag{2}$$

where v_i is the velocity of molecule i, $1 \leqslant i \leqslant N$ and $\langle \cdots \rangle$ indicates an average over time origins. The function $C_v(t)$ is used to calculate the self-diffusion coefficient, D

$$D = \frac{1}{3}\int_0^{t_c} C_v(t)(1 - t/t_c)\, \mathrm{d}t \qquad t_c \to \infty \tag{3}$$

where we have used up to $t_c = 40\sigma(m/\epsilon)^{1/2}$ for the cut-off of the time correlation function (Allen and Tildesley 1989). The diffusion coefficient can also be obtained using the Einstein relationship. Consider the mean square displacement, $W(t)$, of a representative particle in the fluid

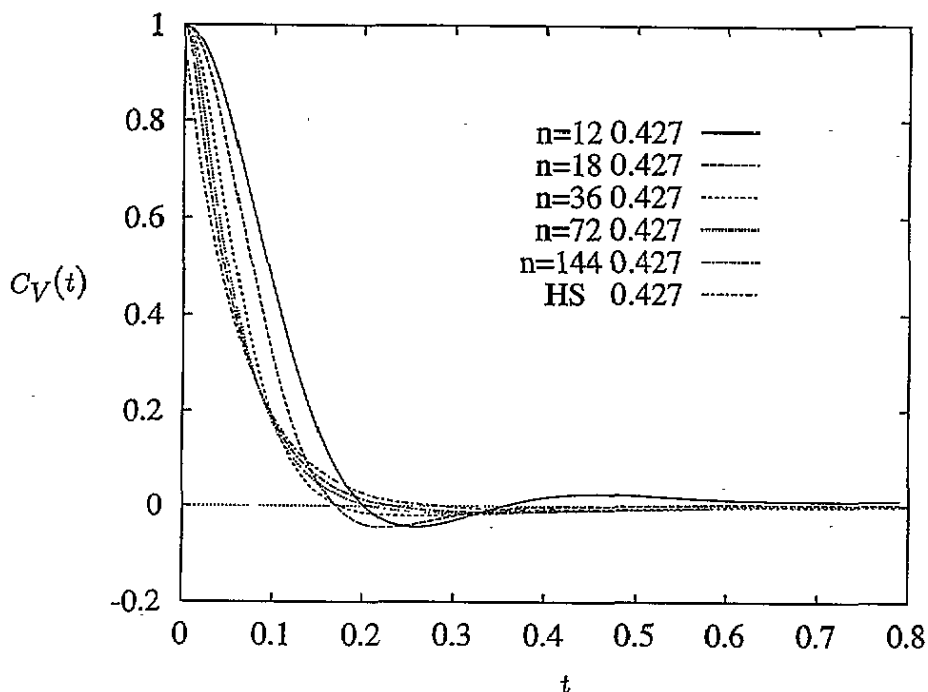$$W(t) = \frac{1}{6}\langle (r(t) - r(0))^2\rangle. \tag{4}$$

Figure 2. The velocity autocorrelation functions for the soft and hard spheres.

The rate of change of $W(t)$ gives the self-diffusion coefficient

$$D = \frac{\mathrm{d}\langle W(t)^2 \rangle}{\mathrm{d}t} \qquad t \to \infty. \tag{5}$$

We find that (5) converges more rapidly to the asymptotic limit than another expression, $W(t)^2/t$. A Green–Kubo expression has been used to compute the shear viscosity via the shear stress, P_{xy}, time autocorrelation function, $C_s(t)$, defined as

$$C_s(t) = \langle P_{xy}(0)P_{xy}(t) \rangle \tag{6}$$

where P_{xy} is an off-diagonal element of the pressure tensor

$$P_{\alpha\beta} = \frac{1}{V}\left(\sum_{i=1}^{N} m_i v_{\alpha i} v_{\beta i} + \sum_{i=1}^{N-1}\sum_{j=i+1}^{N} (r_{\alpha ij} r_{\beta ij}/r_{ij})\frac{\mathrm{d}\phi_{ij}}{\mathrm{d}r} \right) \tag{7}$$

where m_i is the mass of the particle and $v_{\alpha i}$ is the α component of its velocity. This method was first used by Levesque *et al* (1974) who applied it to the LJ fluid. The infinite-frequency linear shear modulus is given by $G_\infty = NC_s(0)/\rho k_B T$. The three unique off-diagonal components of the pressure tensor are used to improve the statistics. The shear viscosity, η_s, is related to $C_s(t)$ through

$$\eta_s = \frac{N}{\rho k_B T}\int_0^{t_c} C_s(t)(1 - t/t_c)\,\mathrm{d}t \qquad t_c \to \infty. \tag{8}$$
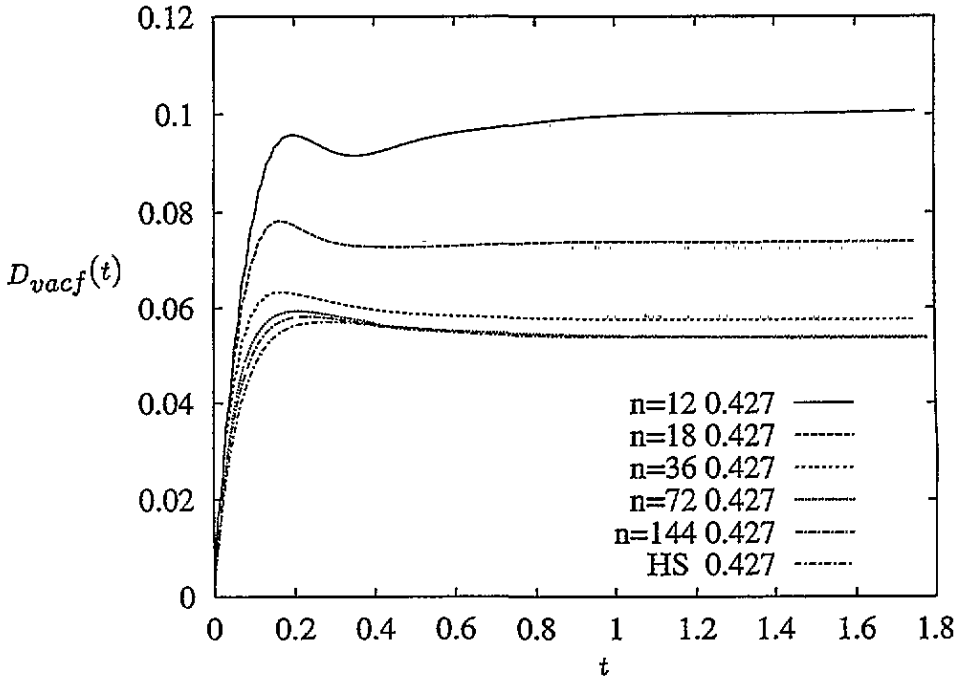
We can write

$$\eta_s = G_\infty \tau_s \tag{9}$$

Figure 3. The time-dependent self-diffusion coefficients for the soft and hard spheres.

where

$$\tau_s = \frac{1}{C_s(0)} \int_0^\infty C_s(t) \, dt. \tag{10}$$

The thermal conductivity was computed using a corresponding heat flux time correlation function as described in Heyes (1988).

The infinite-frequency elastic moduli, the shear, G_∞, and bulk moduli, K_∞, can be computed independently using the Zwanzig and Mountain (1965) expressions

$$G_\infty = \rho k_B T + \frac{2\pi \rho^2}{15} \int_0^\infty g(r) \frac{d}{dr} \left(r^4 \frac{d\phi}{dr} \right) dr \tag{11}$$

and

$$K_\infty = 2\rho k_B T/3 + P + \frac{2\pi \rho^2}{9} \int_0^\infty g(r) r^3 \frac{d}{dr} \left(r \frac{d\phi}{dr} \right) dr \tag{12}$$

where P is the pressure

$$P = \rho k_B T + \frac{2\pi \rho^2}{3} \int_0^\infty g(r) r^3 \frac{d\phi}{dr} \, dr \tag{13}$$

where $g(r)$ is the radial distribution function, and the number density is $\rho = N/V$ for N spheres of diameter σ in volume V. For the inverse power potentials, the pressure and mechanical properties are trivially related to the interaction energy per particle, $u = U/N$

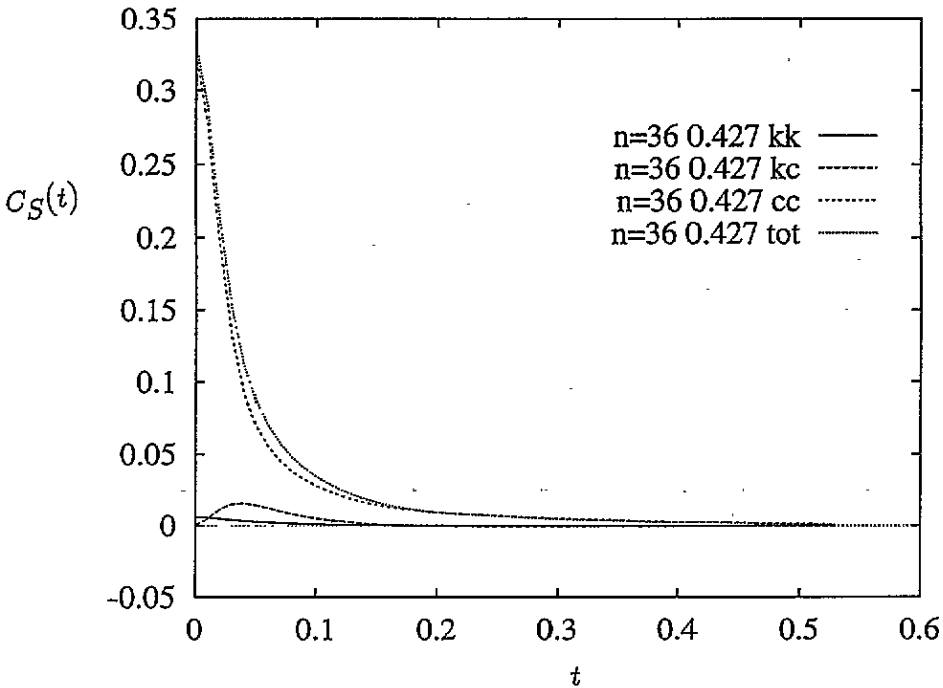$$\langle u \rangle = 2\pi \rho \int_0^\infty g(r) r^2 \phi(r) \, dr. \tag{14}$$

Figure 4. The shear stress autocorrelation function for the $n = 36$ state, resolved into its kinetic (kk), cross (kc) and interaction (cc) components.

For an N-particle periodic system, such as that used in molecular dynamics (MD) or Monte Carlo (MC) simulation

$$\langle u \rangle = \frac{1}{2N} \sum_{i=1}^{N} \sum_{i \neq j} \langle \phi_{ij}(r_{ij}) \rangle. \tag{15}$$

The interaction part of the pressure is given by

$$P^U = n\rho\langle u \rangle/3. \tag{16}$$

The interaction part of the infinite-frequency shear rigidity modulus is given by

$$G_\infty^U = (n^2 - 3n)\rho\langle u \rangle/15 \tag{17}$$

and the interaction part of the infinite-frequency bulk rigidity modulus is given by

$$K_\infty^U = (n^2 + 3n)\rho\langle u \rangle/9. \tag{18}$$

Therefore the n dependence of the elastic moduli is essentially governed by that of the interaction energy. In the limit of $n \to \infty$ we found that $\langle u \rangle \propto n^{-1}$ as predicted by Rowlinson (1964) using a perturbation about the hard-sphere fluid. This result introduced in (17) and (18) indicates an $\sim n$ divergence of the infinite-frequency shear and bulk moduli as $n \to \infty$. Unresolved questions include (a) how do the time correlation functions and their derived transport coefficients approach the hard-sphere limit (in particular their components for N-dependent properties such as viscosity) and (b) how large does n have to be in order

to obtain fluid physical properties statistically indistinguishable from the hard-sphere case. In the next section we describe simulations carried out to answer these questions.

2. The simulations

We carried out extremely long equilibrium molecular dynamics simulations using a series of potentials with $n = 12, 18, 36, 72, 144$, and $n = \infty$ (using an independently written hard-sphere MD code) on $N = 108$ systems, for $\sim 10^6$ timesteps, Δt, of magnitude typically 0.01–0.002 in reduced units of $\sigma(m/\epsilon)^{1/2}$. With the $n = 144$ system, simulations carried out with $\Delta t = 0.0003$ were found to give statistically indistinguishable results from simulations with $\Delta t = 0.001$. There is a practical limit on how large n can be, without the simulation time steps becoming too small, which limits the ability to explore phase space in a reasonable amount of computer time. For N hard spheres in volume V, we define a reduced number
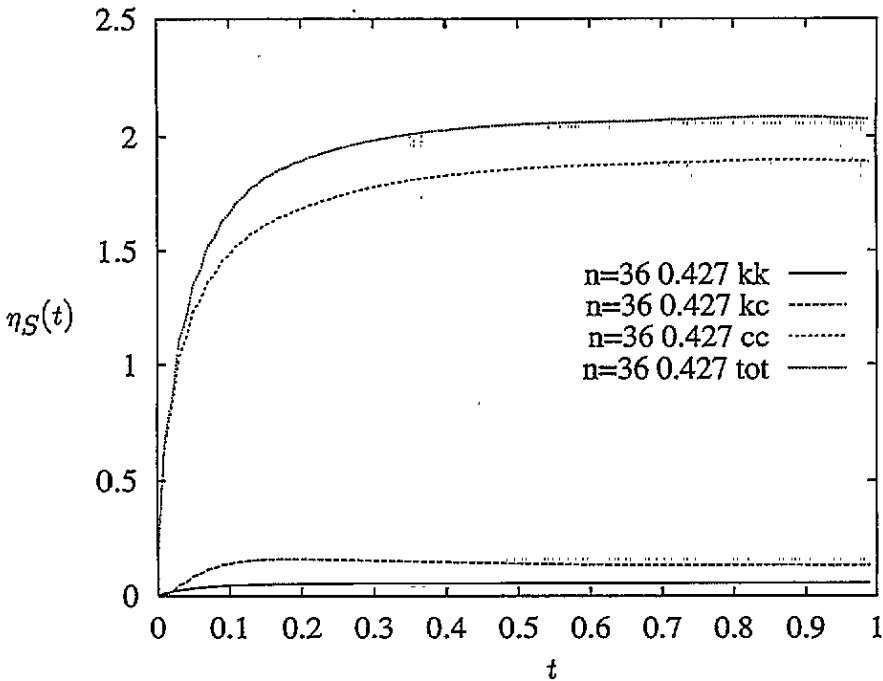

Figure 5. The time-integrated viscosity corresponding to the $C_s(t)$ of figure 4.

density, $\rho = N\sigma^3/V$. The reduced number density of particles can also be defined in terms of a particle volume fraction, $v_f = \pi\rho\sigma^3/6$. We have used the value $v_f = 0.427$ here which corresponds to a reduced number density of $\rho = 0.81551$ (or $V/V_0 = 1.734$ using the notation of Alder *et al* 1970). This value was chosen because it is quite close to the fluid–solid density ($v_f = 0.498$). As the maximum fluid density is approached the system manifests longer-lived 'tails' in the time correlation functions, which make the evaluation of transport coefficients difficult by Green–Kubo formulae. The temperature was $k_B T/\epsilon = 1.0$ for all simulations. The Verlet algorithm was used. All quantities are given in terms of the

usual particle-based units (i.e. σ for length, ϵ for energy and the mass of the particle, m for mass). A summary of the most important computed properties is given in table 1. In figure 1, we show the pair radial distribution function for varying values of the exponent, n, comparing these with hard-sphere MD results. As the potential becomes stiffer, the $g(r)$ increasingly resembles a hard-sphere $g(r)$ as $r \to \sigma$. Using $n = 144$, the highest value of n chosen, there is still a noticeable difference from the HS result in the first peak height (4.29 for the HS case versus 3.49 for $n = 144$). Also in table 1 we note that the value of $\langle u \rangle$ is not zero for $n = 144$, indicating a departure from the hard-sphere limit even at this high value of n. Table 1 gives the $\langle u \rangle$ for the MD simulations. Rowlinson (1964) expanded the

Table 1. Summary of properties for the inverse power fluids at a reduced density of $\rho = 0.81551$ and $k_B T/\epsilon = 1.0$. Key: $Z = PV/Nk_B T$. The interaction energy per particle, $\langle u \rangle$, is defined by (15) for the inverse power potentials of (1) with the n values given below. The hard-sphere thermal conductivity is from the Enskog formula using the $g(\sigma)$ at $N = 108$ and using the correction factor of Alder *et al* (1970). The statistical uncertainty in the MD viscosity and thermal conductivity is estimated to be $\simeq 3\%$ and $\simeq 1\%$ for the self-diffusion coefficient.

	$n = 12$	$n = 18$	$n = 36$	$n = 72$	$n = 144$	$n = \infty$
NT	2107 000	1592 500	8660 00	2717 500	2229 300	—
t_{sim}	21 070	15 925	8660.0	5435.0	4458.6	603
Z	8.701	8.897	8.806	8.537	8.411	8.110
u	1.928	1.318	0.651	0.315	0.160	0
G_∞^U	11.32	19.35	42.06	84.96	176.25	∞
K_∞^U	31.45	45.14	82.85	153.92	306.25	∞
η_s^{kk}	0.0787	0.0644	0.0576	0.0484	0.0451	0.0460
η_s^{kc}	0.0454	0.0907	0.1398	0.1447	0.1696	0.1902
η_s^{cc}	0.9818	1.334	2.031	2.096	2.218	2.358
η_s	1.106	1.489	2.229	2.289	2.432	2.594
κ	5.033	5.6338	6.6194	7.2328	7.5407	7.932
D_{vacf}	0.102	0.0738	0.0577	0.0539	0.0537	0.0536
D_{msd}	0.101	0.0738	0.0577	0.0541	0.0538	0.0553

thermodynamic properties of soft-sphere systems about the hard-sphere limit in powers of n^{-1}. In the $n^{-1} \to 0$ limit for inverse power potentials this is $\langle u(n) \rangle \to 3Z_\infty/n\beta$, where Z_∞ is the compressibility factor of the hard-sphere system. This allows a comparison to be made with the simulation $\langle u \rangle$. Using the Carnahan–Starling hard-sphere equation of state for hard spheres (Carnahan and Starling 1969), the proportionality constant is $K(v_f) = 3k_B T Z_\infty$, and for $v_f = 0.427$ has the value $K(v_f) = 21.42$. This relation predicts for $n = 12, 18, 36, 72$ and 144 the values of $u = 1.785, 1.190, 0.595, 0.298$ and 0.149 respectively which agree reasonably well with the simulation values given in table 1.

We now turn to the transport coefficients. In figure 2 the velocity autocorrelation functions for the inverse power and hard-sphere fluids are presented. As the interaction becomes harder, the negative 'backscattering' region at $t \sim 0.2$–0.3 becomes less pronounced. The diffusion coefficients using (3) (shown in figure 3) and also from the associated mean square displacements using (5) are given in table 1. The diffusion coefficients derived decrease in magnitude with increasing n. We conclude that for $n \geqslant 72$ the value of D is statistically indistinguishable from the hard-sphere value. The density dependence of the self-diffusion coefficient of the hard-sphere fluid has been studied, with
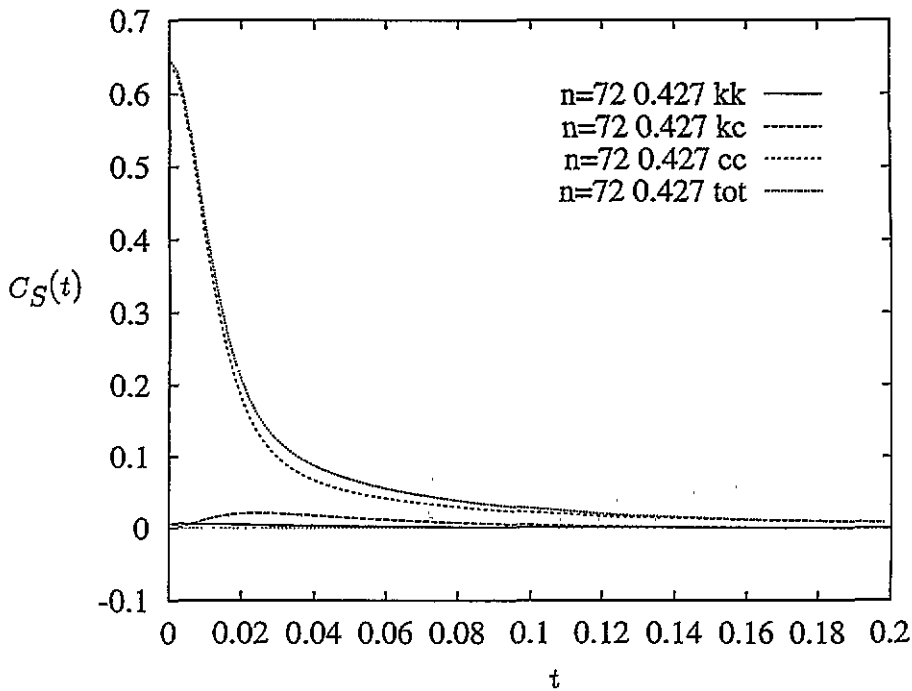
Figure 6. Same as figure 4, for the $n = 72$ case.

several analytic fits for $D(\rho)$ now available in the literature. A fit to simulation data given by Speedy (Speedy 1987) is

$$D = D_{00} \left(1 - \left(\frac{\rho}{1.09}\right)\right) (1 + \rho^2(0.4 - 0.83\rho^2)).\qquad(19)$$

Erpenbeck and Wood (1991) have fitted their MD hard-sphere simulation data to the expression

$$D = D_E(1 + a_1\rho + a_2\rho^2 + a_3\rho^3)\qquad(20)$$

where $a_1 = 0.038\,208\,154$, $a_2 = 3.182\,808$ and $a_3 = -3.868\,771\,766$. Both (19) and (20) include a reference self-diffusion coefficient. The diffusion coefficient for an ideal hard-sphere gas, D_{00}, is determined from kinetic theory to be

$$D_{00} = 3(k_B T/\pi m)^{1/2}/8\rho\sigma^2\qquad(21)$$

and D_E is the Enskog theory extension of these basic assumptions to finite density

$$D_E = 1.018\,96D_{00}/g(\sigma)\qquad(22)$$

where $g(\sigma)$ is the value of the pair radial distribution function at the contact of the spheres. Using the Carnahan–Starling equation of state for $g(\sigma)$, equations (19) and (20) give self-diffusion coefficients of 0.0587 and 0.0664 respectively. The HS simulation carried out here using $N = 108$ gives $D = 0.054$, which is in excellent agreement with the continuous potential D values for $n > 72$. Erpenbeck and Wood studied up to $N = 4732$, so it is reasonable that the self-diffusion coefficient from this work should be a little lower
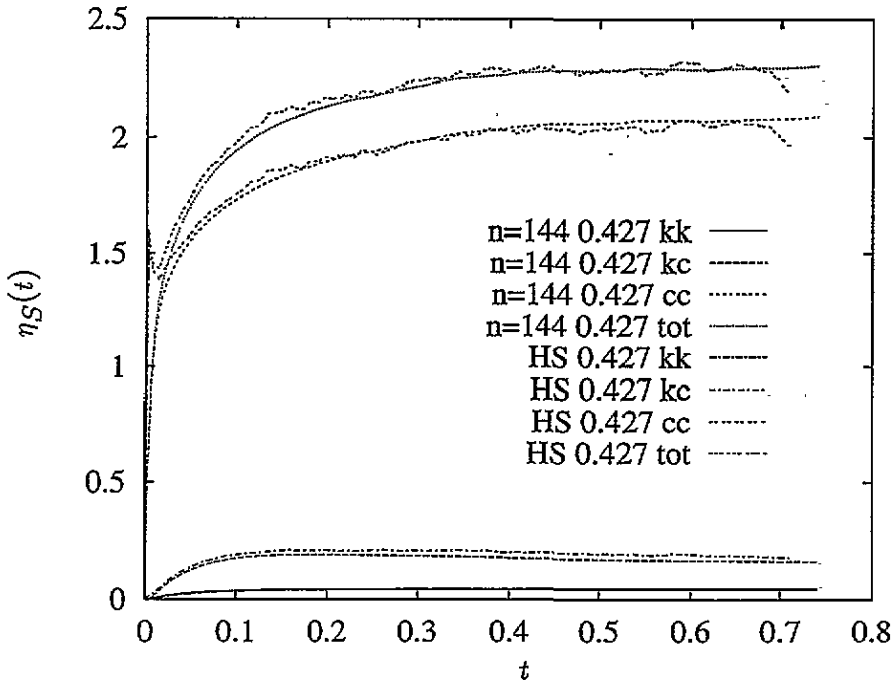
Figure 7. A comparison between the $n = 144$ time-integrated viscosity components compared with the corresponding hard-sphere case.
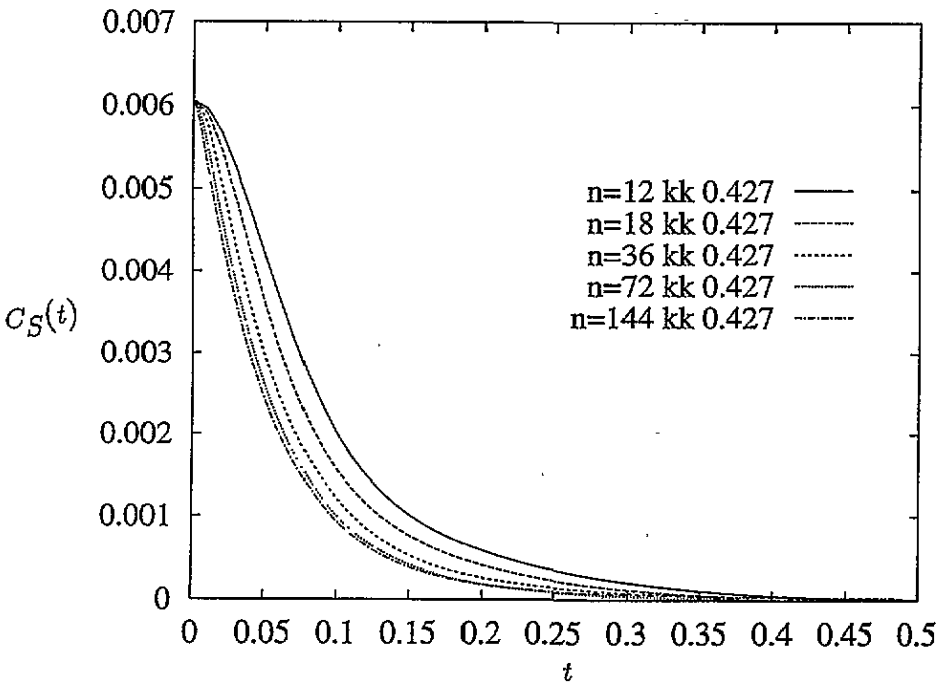

Figure 8. The purely kinetic, kk, component of the shear stress autocorrelation function for the n values considered.
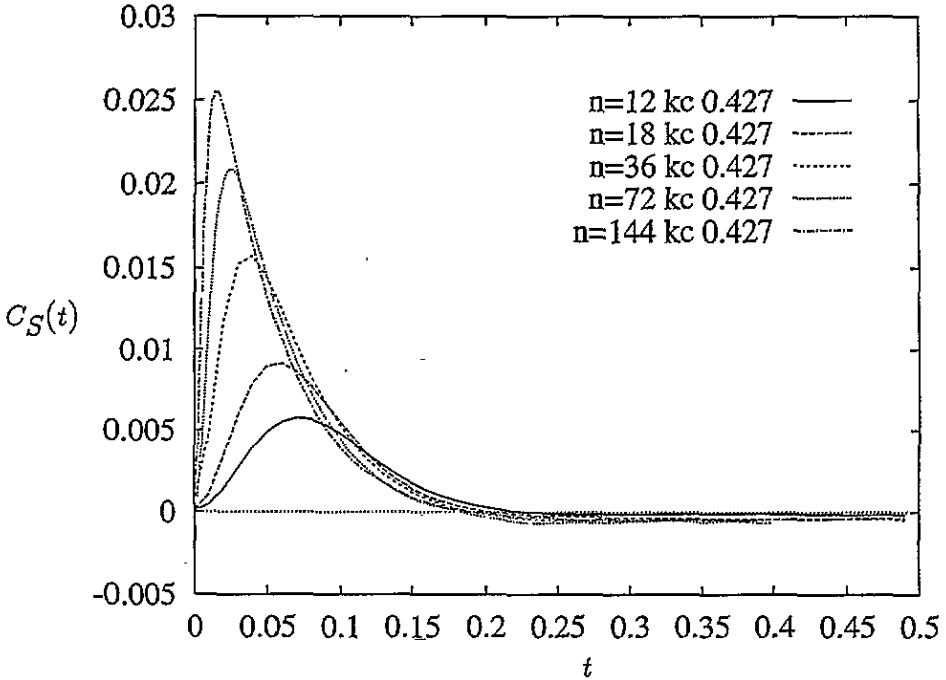
Figure 9. The cross term, kc, component of the shear stress autocorrelation function for the n values considered.

than these formulae predict. As we only considered $N = 108$, the present simulation values for D for the hard-sphere are probably a little small compared with the value in the thermodynamic limit. However, the main purpose of this work is to investigate the approach of the inverse power fluids to the hard-sphere limit. So the same degree of N dependency should be present in all the systems considered, to a good approximation, as all the simulations were performed with the same N. The $C_s(t)$ components of the $n = 36$ state are given in figure 4. It is seen that the interaction or, using the notation of Alder *et al* (1970), the cc component of the stress autocorrelation function is the most important term, especially at short and long times. In the intermediate-time regime the cross, kc, term makes a significant contribution to the total value of $C_s(t)$. In figure 5 we show the integrated $C_s(t)$ giving the time-dependent shear viscosity, $\eta_s(t)$. Figure 6 shows the components and total $C_s(t)$ for the $n = 72$ state. In figure 7 we make a comparison between the components of the integrated $C_s(t)$ for the $n = 144$ state (which is the closest to the hard-sphere interaction we considered) and those of the hard-sphere system itself, the latter using the numerical differentiation procedure developed by Alder *et al* (1970). Numerical differentiation is particularly difficult and prone to statistical fluctuations as $t \to 0$, which gives rise to the observed noisy peak in the hard-sphere cc components in the $t \to 0$ limit. There is excellent agreement for the kk (purely kinetic) component of $\eta_s(t)$ between the $n = 144$ and hard-sphere system. The kc and cc hard-sphere components are higher than the $n = 144$ functions but follow the same qualitative time dependence. Taking the $t \to \infty$ limit, the shear viscosity increases with n, but is still $\simeq 6\%$ smaller than the
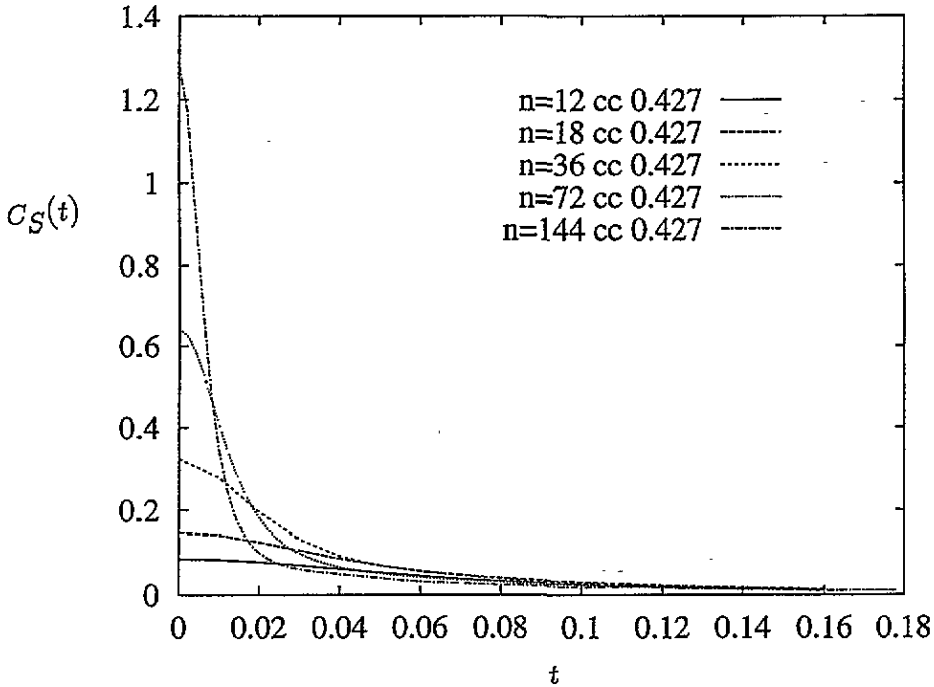
Figure 10. The interaction term, *cc*, component of the shear stress autocorrelation function for the *n* values considered.

hard-sphere limit for $n = 144$. In contrast to the self-diffusion coefficients, therefore, there are still significant differences in the value of the shear viscosity between $n = 144$ and the hard-sphere system. Clearly, a much higher value of n is required for this quantity, in contrast to the situation for the self-diffusion coefficient. In the following figures we present the n dependence of the components of $C_s(t)$ (the comparable hard-sphere functions are statistically very poor as it requires a second derivative of the numerical data for them to be obtained). In figure 8 we show the kk component of $C_s(t)$. This function decays more rapidly with time as n increases. The cross or kc component increases in magnitude and the peak shifts to shorter times as n increases (figure 9). The interaction or cc component, shown in figure 10, increases in magnitude and becomes more short-ranged in time as n increases. Interestingly, the long-time tails of the kc and cc components converge so that they superimpose for $t \simeq 0.1$ and become therefore effectively n independent. It is only at 'short' times (i.e. $t < 0.1$) that the n dependence is significant. Hard-sphere MD calculations of the shear viscosity using time correlation functions by Erpenbeck and Wood (1981) and of the self-diffusion coefficient from velocity autocorrelation functions by Erpenbeck and Wood (1985, 1991) have tested the mode coupling theory prediction of a $\propto t^{-3/2}$ long-time tail. They found reasonable agreement for times ~ 4 in our units. However, the main failing of this theory is that it does not account for the dominance of the direct (cc and kc) interaction contribution to the time correlation function. The mode coupling theory erroneously predicts that these are asymptotically zero compared to the kk part.
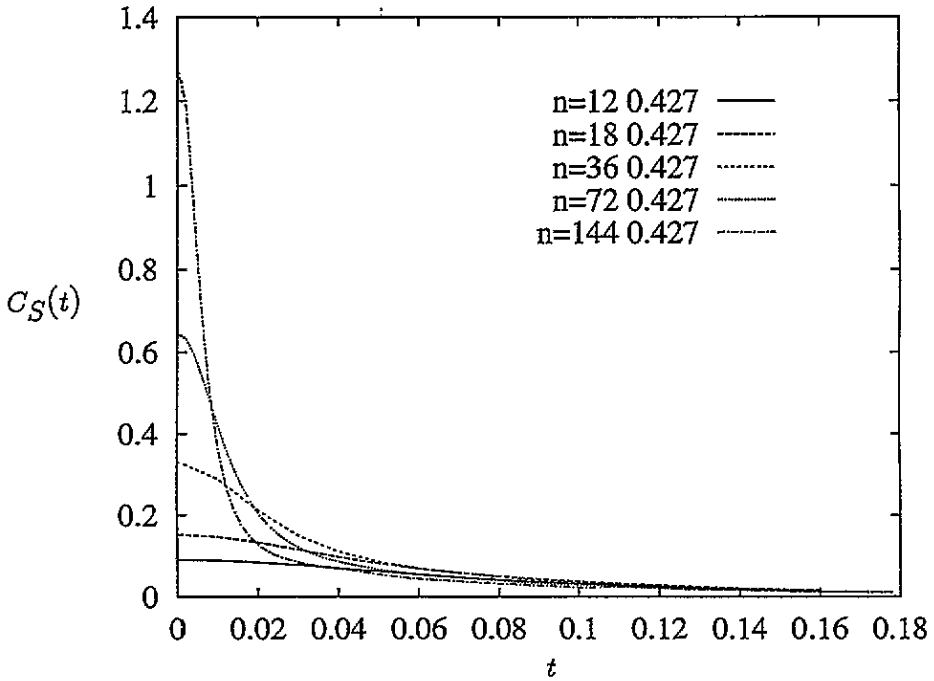
Figure 11. The total shear stress autocorrelation function for the n values considered.
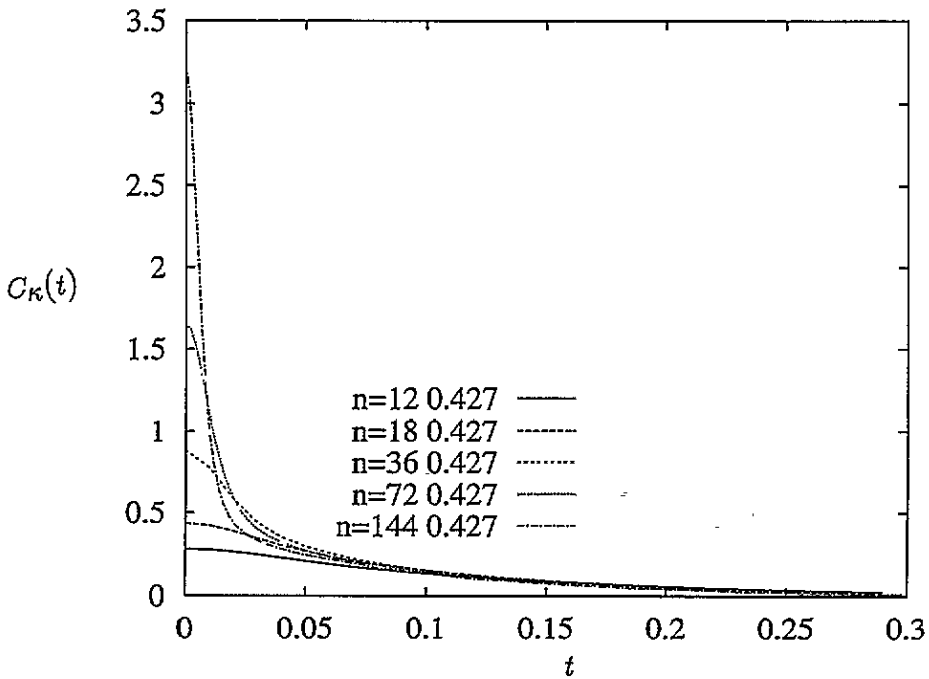

Figure 12. The total heat flux correlation function for the n values considered.

3. Conclusions

Following on from a previous publication (Heyes and Aston 1994) which was devoted to elastic moduli of inverse power fluids, we have explored here the effect of potential steepness on the transport coefficients of model fluids. In figure 11, we show the total $C_s(t)$, which reveals the dominance of the cc term in determining the total function. This trend is also manifest in the corresponding time correlation functions for the thermal conductivity, κ, as revealed in figure 12. We have focused on the approach to the hard-sphere limit. We have found that, even with an inverse power potential index, $n = 144$, there are still noticeable differences in some of the properties when compared with the hard-sphere fluid at the same number density. The compressibility factor, shear viscosity and thermal conductivity are some 5–10% lower that the hard-sphere value, whereas the self-diffusion agrees well for $n > 72$.

References

Alder B J, Gass D M and Wainwright T E 1970 *J. Chem. Phys.* **53** 3813
Allen M P and Tildesley D J 1987 *Computer Simulation of Liquids* (Oxford: Oxford University Press) p 60
Carnahan N F and Starling K E 1969 *J. Chem. Phys.* **51** 635
Erpenbeck J J and Wood W W 1981 *J. Stat. Phys.* **24** 455
—— 1985 *Phys. Rev.* A **32** 412
—— 1991 *Phys. Rev.* A **43** 4254
Heyes D M 1988 *Phys. Rev.* B **37** 5677
Heyes D M and Aston P J 1994 *J. Chem. Phys.* **100** 2149
Langston P A, Tüzün U and Heyes D M 1994 *Chem. Eng. Sci.* **49** 1259
Levesque D, Verlet L and Kurkijarvi J 1973 *Phys. Rev.* A **7** 1690
Melrose J R and Heyes D M 1993 *J. Chem. Phys.* **98** 5873
Rowlinson J S 1964 *Mol. Phys.* **8** 107
Speedy R J 1987 *Mol. Phys.* **62** 509
Zwanzig R and Mountain R D 1965 *J. Chem. Phys.* **43** 4464